Received: 27 April 2023 | Revised: 11 July 2023 | Accepted: 18 July 2023

DOI: 10.1002/psp4.13023

ARTICLE

# Physiologically-based pharmacokinetic modeling for investigating the effect of simeprevir on concomitant drugs and an endogenous biomarker of OATP1B

**Shinji Nakayama**[1] | **Kota Toshimoto**[2,3] | **Shinji Yamazaki**[4] | **Jan Snoeys**[5] | **Yuichi Sugiyama**[3,6]

[1]DMPK Research Laboratories, Shoyaku, Innovative Research Division, Mitsubishi Tanabe Pharma Corporation, Yokohama, Kanagawa, Japan

[2]Systems Pharmacology, Non-Clinical Biomedical Science, Applied Research and Operations, Astellas Pharma Inc., Ibaraki, Japan

[3]Sugiyama Laboratory, RIKEN Cluster for Science, RIKEN, Yokohama, Kanagawa, Japan

[4]Drug Metabolism and Pharmacokinetics, Janssen Research and Development, LLC, San Diego, California, USA

[5]Drug Metabolism and Pharmacokinetics, Janssen Research and Development, Beerse, Belgium

[6]Laboratory of Quantitative System Pharmacokinetics/Pharmacodynamics, Josai International University (JIU), Tokyo, Japan

**Correspondence**
Yuichi Sugiyama, Laboratory of Quantitative System Pharmacokinetics/Pharmacodynamics, School of Pharmacy, Josai International University, 2-3-11 Hirakawa-cho, Chiyoda-ku, Tokyo 102-0093, Japan.
Email: y-sugiyama@jiu.ac.jp

## Abstract

The orally available anti-hepatitis C virus (HCV) drug simeprevir exhibits nonlinear pharmacokinetics at the clinical doses due to saturation of cytochrome P450 (CYP) 3A4 metabolism and organic anion transporting peptide (OATP) 1B mediated hepatic uptake. Additionally, simeprevir increases exposures of concomitant drugs by CYP3A4 and OATP1B inhibition. The objective of this study was to develop physiologically-based pharmacokinetic (PBPK) models that could describe drug–drug interactions (DDIs) of simeprevir with concomitant drugs via CYP3A4 and OATP1B inhibition, and also to capture the effects on coproporphyrin-I (CP-I), an endogenous biomarker of OATP1B. PBPK modeling estimated unbound simeprevir inhibitory constant ($K_i$) of 2.89 μM against CYP3A4 in the DDI results between simeprevir and midazolam in healthy volunteers. Then, we analyzed the DDIs between simeprevir and atorvastatin, a dual substrate of CYP3A4 and OATP1B, in healthy volunteers, and unbound $K_i$ against OATP1B was estimated to be 0.00347 μM. Finally, we analyzed the increase in the blood level of CP-I by simeprevir to verify the $K_{i,OATP1B}$. Because CP-I was measured in subjects with HCV with various hepatic fibrosis state, Monte Carlo simulation was performed to involve the decreases in expression levels of hepatic CYP3A4 and OATP1B and their interindividual variabilities. The PBPK modeling coupled with Monte Carlo simulation using the $K_{i,OATP1B}$ value obtained from atorvastatin study reasonably recovered the observed relationship between CP-I and simeprevir blood levels. In conclusion, the simeprevir PBPK model developed in this study can quantitatively describe the increase in exposures of concomitant drugs and an endogenous biomarker via inhibition of CYP3A4 and OATP1B.

---

This is an open access article under the terms of the Creative Commons Attribution-NonCommercial-NoDerivs License, which permits use and distribution in any medium, provided the original work is properly cited, the use is non-commercial and no modifications or adaptations are made.
© 2023 The Authors. *CPT: Pharmacometrics & Systems Pharmacology* published by Wiley Periodicals LLC on behalf of American Society for Clinical Pharmacology and Therapeutics.

## Study Highlights

**WHAT IS THE CURRENT KNOWLEDGE ON THE TOPIC?**

Simeprevir, an inhibitor of CYP3A4 and OATP1B, increases the exposures of concomitant drugs (midazolam and atorvastatin) in healthy subjects and an endogenous biomarker of OATP1B, CP-I, in patients with HCV.

**WHAT QUESTION DID THIS STUDY ADDRESS?**

Can physiologically-based pharmacokinetic (PBPK) model analysis of simeprevir successfully capture the interactions with concomitant drugs and CP-I both in healthy subjects and patients with HCV?

**WHAT DOES THIS STUDY ADD TO OUR KNOWLEDGE?**

The simeprevir PBPK model coupled with Monte Carlo simulation can adequately recover the interactions with concomitant drugs and CP-I. Our analysis reveals that not only OATP1B increases inhibition by simeprevir but also decreases in expression levels of hepatic CYP3A4 and OATP1B due to progression of liver fibrosis can affect the relationship between simeprevir and CP-I blood levels in patients with HCV.

**HOW MIGHT THIS CHANGE DRUG DISCOVERY, DEVELOPMENT, AND/OR THERAPEUTICS?**

PBPK models taking interindividual difference and diseased conditions into account can reasonably describe the drug–drug and -endogenous biomarker interactions and will help the drug development and/or therapeutics.

# INTRODUCTION

Simeprevir is an orally available drug for the treatment of hepatitis C virus (HCV) by inhibiting NS3/4A protease. Plasma exposures after single oral dose of simeprevir at the dose range from 50 mg to 600 mg have been evaluated in a phase I clinical trial in healthy volunteers (HVs). Plasma exposures increased dose-proportionally at the doses of 50–100 mg and greater than dose-proportionally at the doses of 150–600 mg.[1] Simeprevir is a substrate of cytochrome P450 (CYP) 3A4, organic anion transporting peptide (OATP) 1B, and p-glycoprotein (P-gp).[1,2] An analysis of simeprevir pharmacokinetics was performed using a physiologically-based pharmacokinetic (PBPK) model, and the results suggested that the saturation of CYP3A4 metabolism and the OATP1B mediated hepatic uptake were major factors for the nonlinear pharmacokinetics.[1] On the other hand, because a mass balance study demonstrated that the fraction absorbed of simeprevir at the dose of 50 mg was high (0.75),[3] it was considered that the impact of saturation of the P-gp mediated efflux at the intestinal tract on the nonlinear pharmacokinetics was limited.

It has been reported that co-administration of itraconazole, a potent CYP3A4 inhibitor, and rifampicin, an OATP1B inhibitor, increased the plasma exposure of simeprevir at the dose of 0.016 mg/kg.[4] In addition, it has been also reported that co-administration of ritonavir, erythromycin, and cyclosporine increased the plasma exposure of simeprevir at the dose of 150 mg, and their mechanisms were considered to be inhibition of CYP3A4, OATP1B, and P-gp.[5]

Simeprevir is not only a substrate but also an inhibitor of CYP3A4 and OATP1B. In a clinical drug–drug interaction (DDI) study in HVs, simeprevir at the therapeutic dose of 150 mg q.d. increased the plasma area under the plasma concentration-time curve (AUC) of oral midazolam, a CYP3A4 probe substrate, by 1.45-fold. On the other hand, there was no impact of concomitant dosing of simeprevir on the intravenous midazolam AUC. This was likely due to simeprevir mainly inhibiting CYP3A4 in the intestinal tract, instead of liver. The 2.12-fold increase in the AUC of atorvastatin, a dual substrate of CYP3A4 and OATP1B, has been reported with co-administration of simeprevir at the dose of 150 mg q.d.[5] In addition, plasma coproporphyrin-I (CP-I), an endogenous substrate of OATP1B, was measured in a clinical phase III study in subjects with HCV,[6] and it was confirmed that plasma CP-I concentrations increased where plasma simeprevir concentrations exceeded 3 μM, suggesting that OATP1B inhibition by simeprevir was involved in the increase in plasma CP-I concentrations.[7] It has also been reported that hepatic OATP1B expression level decreased with the progression of hepatic fibrosis in patients with HCV.[8] Therefore, it is considered that decreases in OATP1B expression levels due to progression of hepatic fibrosis as well as OATP1B inhibition by simeprevir can be involved in the increase in plasma CP-I concentration observed in the clinical study.

Modeling approach is a powerful tool to predict and understand complex DDI quantitatively.[9–14] PBPK model analysis with Monte Carlo sampling can describe not only average but also individual DDI. Whereas the PBPK model analysis for DDI of simeprevir as a victim drug has already been performed,[1] the quantitative model analysis investigating a series of DDIs of simeprevir as a perpetrator has not yet been done yet. In this study, the PBPK model analysis was performed on a series of DDIs in which simeprevir is a perpetrator drug. For highly lipophilic drugs, such as simeprevir,[1] it has been reported that inhibitory concentration of drug metabolizing enzymes and transporters determined by in vitro experiments may underpredict the magnitude of DDI in vivo due to high adsorption to experimental materials and protein components.[15] Therefore, top-down estimation using PBPK modeling was performed to obtain in vivo inhibitory constant ($K_i$) of simeprevir against CYP3A4 and OATP1B by analyzing DDIs with midazolam and atorvastatin. Then, the effect of simeprevir on plasma CP-I level was simulated to verify $K_i$ against OATP1B ($K_{i,OATP1B}$) using constructed PBPK model coupled with Monte Carlo sampling.

# METHODS

## Development of simeprevir PBPK model

The PBPK model structure and parameters of simeprevir are shown in Figure 1a and Table 1. The physiological parameters are shown in Table S1. The model code is available in the previous report.[16] The liver in this model consisted of extracellular and intracellular compartments, which were further divided into five parts to give a structure similar to the dispersion model.[17] The reported overall intrinsic clearance ($CL_{int,all}$), $R_{dif}$ ($PS_{dif,inf}/PS_{act,inf}$), $\gamma$ ($PS_{dif,inf}/PS_{dif,eff}$), and $\beta$ (($CL_{int,met}+CL_{int,bile}$)/($PS_{dif,eff}+CL_{int,met}+CL_{int,bile}$)) were used.[4] The reported kinetic metabolite ($K_m$) for CYP3A4 metabolism and OATP1B mediated hepatic uptake were also used to capture the nonlinear pharmacokinetics.[1] Enterohepatic circulation was described by connecting the hepatocytes and intestinal lumen compartments with three tandem transit compartments. The intestinal tract was divided into luminal and cellular compartments,[18] and intestinal CYP3A4 metabolism of simeprevir was considered. Muscle, adipose, and skin were selected as the distribution organs, and the

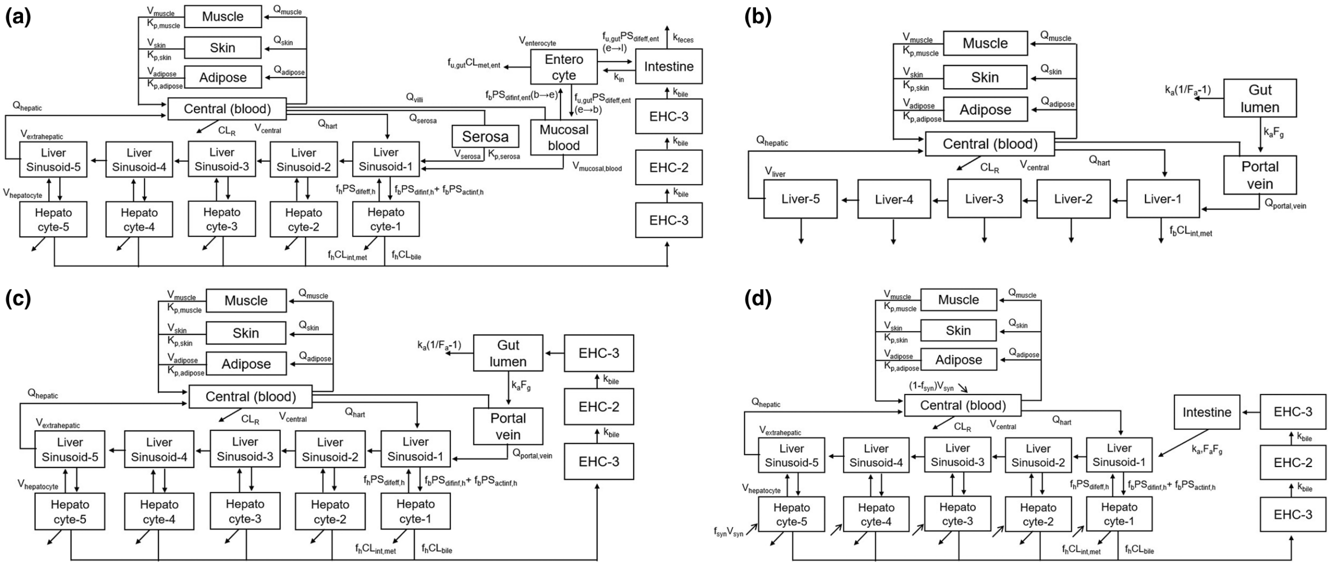
(a)
Muscle
Skin
Adipose
Central (blood)
Entero cyte
Intestine
Mucosal blood
Serosa
EHC-3
EHC-2
EHC-3
Liver Sinusoid-5
Liver Sinusoid-4
Liver Sinusoid-3
Liver Sinusoid-2
Liver Sinusoid-1
Hepato cyte-5
Hepato cyte-4
Hepato cyte-3
Hepato cyte-2
Hepato cyte-1
Q_hepatic
Q_villi
Q_serosa
Q_hart
CL_R
k_bile
k_feces
k_in
f_hCL_int,met
f_bCL_bile
(b)
Gut lumen
Portal vein
Liver-5
Liver-4
Liver-3
Liver-2
Liver-1
k_a(1/F_a-1)
k_aF_g
Q_portal,vein
f_bCL_int,met
(c)
Gut lumen
Portal vein
EHC-3
EHC-2
EHC-3
(d)
Intestine
EHC-3
EHC-2
EHC-3
(1-f_syn)V_syn
f_synV_syn
k_aF_aF_g

**FIGURE 1** Structures of PBPK model of simeprevir (a), midazolam (b),[9] atorvastatin (c),[22] and coproporphyrin-I (d).[22,24] The liver compartment was further divided into five subcompartments to construct a model similar to the dispersion model.[17] PBPK models for simeprevir, atorvastatin, and coproporphyrin-I were developed assuming a perfusion rate-limited distribution, whereas a rapid equilibrium for midazolam. Enterohepatic circulation was incorporated for simeprevir, atorvastatin and coproporphyrin-I. Portal vein blood flow was divided into mucosal and serosal blood flow for simeprevir.[18] $CL_{bile}$, intrinsic clearance of biliary excretion; $CL_{int,met}$, intrinsic clearance of hepatic metabolism; $CL_R$, renal clearance; $CL_{met,ent}$, intrinsic clearance of intestinal metabolism; $F_a$, fraction absorbed; $F_g$, intestinal metabolic availability; $f_b$, protein unbound fraction in blood; $f_h$, hepatic protein unbound fraction; $f_{u,gut}$, unbound fraction in enterocyte; $f_{syn}$, fraction of CP-I biosynthesis in the liver; $k_a$, absorption rate constant; $K_p$, tissue/blood concentration ratio; $k_{bile}$, transit rate constant for enterohepatic circulation; PBPK, physiologically-based pharmacokinetic; $PS_{actinf,h}$, active uptake intrinsic clearance on sinusoidal membrane; $PS_{difinf,ent}$, influx clearance by passive diffusion through basolateral membranes from the mucosal blood to the enterocyte; $PS_{difinf,h}$, influx intrinsic clearance by passive diffusion through sinusoidal membrane; $PS_{difeff,ent}$, efflux clearance by passive diffusion through a basolateral membrane from the enterocyte to the mucosal blood; $PS_{difeff,h}$, efflux intrinsic clearance by passive diffusion through sinusoidal membrane; $Q_{tissue}$, blood flow rate in tissue; $V_{syn}$, rate of CP-I biosynthesis in the whole body; $V_{tissue}$, tissue volume.

**TABLE 1** Fixed and optimized PBPK model parameters of simeprevir.

| Parameter | Fixed | Optimized, CV% (Initial) | Unit | References |
|---|---|---|---|---|
| $P_{\mathrm{eff}}$ | – | 0.189, 7.04% (0.504) | $10^{-4}$cm/s | – |
| AR | – | 4.79, 2.79% (1.00) | – | – |
| $f_{\mathrm{b}}$ | 0.00139 | – | – | 4 |
| $R_{\mathrm{B}}$ | 0.72 | – | – | 4 |
| $f_{\mathrm{h}}$ | 0.0147 | – | – | 4 |
| $f_{\mathrm{u,gut}}$ | 0.095 | – | – | 19,20 |
| $K_{\mathrm{p,skin}}$ | 0.389 | – | – | 4 |
| $K_{\mathrm{p,muscle}}$ | 0.09 | – | – | 4 |
| $K_{\mathrm{p,adipose}}$ | 0.0743 | – | – | 4 |
| $K_{\mathrm{p,gut}}$ | 0.222 | – | – | 19,20 |
| $K_{\mathrm{m,u,CYP3A4}}$ | 7.5 | – | µg/L | 1 |
| $V_{\mathrm{max,CYP3A4}}$ | 1740 | – | µg/h | Calculated from 1 and 4 |
| $f_{\mathrm{m,CYP3A4}}$ | 0.81 | – | – | 4 |
| $K_{\mathrm{m,u,OATPIB}}$ | 2.25 | – | µg/L | 1 |
| $V_{\mathrm{max,OATP1B}}$ | 70,500 | – | µg/h | Calculated from 1 and 4 |
| $\mathrm{CL_R}$ | 0 | – | L/h | 4 |
| $\mathrm{CL_{int,all}}$ | 6970 | – | L/h | 4 |
| $R_{\mathrm{dif}}$ | 0.0113 | – | – | 4 |
| $f_{\mathrm{bile}}$ | 0.31 | – | – | 4 |
| $\gamma$ | 0.24 | – | – | 4 |
| $\beta$ | 0.22 | – | – | 4 |
| $K_{\mathrm{i,u,CYP3A4}}$ | – | 2170, 23.9% (89100) | µg/L | – |
| $K_{\mathrm{i,u,OATP1B}}$ | – | 2.60, 6.73% (525) | µg/L | – |

*Note*: $R_{\mathrm{dif}} = \mathrm{PS_{dif,inf}}/\mathrm{PS_{act,inf}}$, $f_{\mathrm{bile}} = \mathrm{CL_{int,bile}}/(\mathrm{CL_{int,met}} + \mathrm{CL_{int,bile}})$, $\gamma = \mathrm{PS_{dif,inf}}/\mathrm{PS_{dif,eff}}$, $\beta = (\mathrm{CL_{int,met}} + \mathrm{CL_{int,bile}})/(\mathrm{PS_{dif,eff}} + \mathrm{CL_{int,met}} + \mathrm{CL_{int,bile}})$.Comparable $\mathrm{CL_{int,all}}$ (10,800 L/h) was reported by Snoeys et al. assuming following scaling parameters (111 pmol CYP3A4/mg microsomal protein, 99 million cells/g liver, 32 mg microsomal protein/g liver and 1799 g liver/body).[1,31,32]

$V_{\mathrm{max,CYP3A4}}$ was calculated by $(1 - f_{\mathrm{bile}}) \cdot \beta \cdot \mathrm{CL_{int,all}} \cdot R_{\mathrm{dif}} \cdot f_{\mathrm{m,CYP3A4}} \cdot \mathrm{K_{m,u,CYP3A4}}/((1 - \beta) \cdot \gamma \cdot \beta \cdot (1 + R_{\mathrm{dif}}))$.

$V_{\mathrm{max,OATP1B}}$ was calculated by $\mathrm{CL_{int,all}} \cdot \mathrm{K_{m,u,OATPIB}}/(\beta \cdot (1 + R_{\mathrm{dif}}))$.

$K_{\mathrm{p,tissue}}$ and $f_{\mathrm{u,gut}}$ were calculated as previously reported by Rodgers and Rowland.[19,20]

$K_{\mathrm{i,u,CYP3A4}}$ of 2170 µg/L corresponds to 2.89 µM, $K_{\mathrm{i,u,OATP1B}}$ of 2.60 µg/L corresponds to 0.00347 µM.

Abbreviations: AR, apical to basolateral intestinal membrane surface area ratio; $\mathrm{CL_{int,all}}$, overall intrinsic hepatic clearance; $\mathrm{CL_{int,bile}}$, intrinsic biliary excretion clearance; $\mathrm{CL_{int,met}}$, intrinsic metabolic clearance; $\mathrm{CL_R}$, renal clearance; CV%, coefficient of variation percentage; $f_{\mathrm{b}}$, blood unbound fraction; EHC, enterohepatic circulation; $f_{\mathrm{u,gut}}$, unbound fraction in enterocytes; $f_{\mathrm{h}}$, unbound fraction in hepatocytes; $f_{\mathrm{m,CYP3A4}}$, fraction metabolized for CYP3A4; $K_{\mathrm{i,u,CYP3A4}}$, unbound inhibition constant against CYP3A4; $K_{\mathrm{i,u,OATP1B}}$, unbound inhibition constant against OATP1B; $K_{\mathrm{m,u,CYP3A4}}$, unbound Michaelis–Menten constant for CYP3A4; $K_{\mathrm{m,u,OATP1B}}$, unbound Michaelis–Menten constant for OATP1B; $K_{\mathrm{p}}$, tissue, tissue to blood tissue partition coefficients; PBPK, physiologically-based pharmacokinetic; $P_{\mathrm{eff}}$, effective permeability; $\mathrm{PS_{act,inf}}$, active uptake intrinsic clearance on sinusoidal membrane; $\mathrm{PS_{dif,eff}}$, efflux intrinsic clearance by passive diffusion through sinusoidal membrane; $\mathrm{PS_{dif,inf}}$, influx intrinsic clearance by passive diffusion through sinusoidal membrane; $R_{\mathrm{B}}$, blood to plasma concentration ratio; $V_{\mathrm{max,CYP3A4}}$, maximum velocity for CYP3A4; $V_{\mathrm{max,OATP1B}}$, maximum velocity for OATP1B.

blood to tissue concentration ratio ($K_{\mathrm{p}}$) in each organ was predicted based on logP, $\mathrm{pK_a}$, and plasma unbound fraction.[19,20] The measured plasma concentrations were converted to blood concentrations by correcting the blood to plasma concentration ratio. The effective permeability ($P_{\mathrm{eff}}$) in the intestinal tract and the passive diffusion ratio between from enterocyte to intestinal lumen and from enterocyte to mucosal blood (AR) were optimized simultaneously to recover the blood concentration-time profiles of simeprevir at the six dose levels from 50 mg to 600 mg. All DDI studies were conducted at a dose level of 150 mg q.d. simeprevir.[5,7] Nonetheless, plasma simeprevir concentrations after once daily dosing at a dose of 150 mg in subjects with HCV were distributed in a wide range (~20–40,000 ng/mL) in the clinical trial investigating the effect on CP-I. Interindividual variability in drug clearance and nonlinear pharmacokinetics may result in this study outcome. Therefore, it was required to describe nonlinear pharmacokinetics and interindividual variability of simeprevir in the present study.

## DDI analysis of simeprevir and midazolam

The effect of simeprevir multiple dose (150 mg q.d.) on the blood concentration-time profiles of midazolam after oral and intravenous administrations were evaluated in healthy subjects.[5] The PBPK model structure and parameters of midazolam are shown in Figure 1b and Table S2. The published PBPK model structure was used.[9] A rapid equilibrium distribution to the liver was assumed. Intestinal absorption was described by $Q_{gut}$ model to take its intestinal metabolism into consideration. The absorption rate constant ($k_a$), $CL_{int,all}$, and scaling factor of $K_p$ ($Y_{Kp}$) were optimized simultaneously to reproduce the time course of midazolam blood concentration after intravenous and oral administration in the absence of simeprevir. Then, we estimated the $K_i$ of simeprevir against CYP3A4 ($K_{i,CYP3A4}$) to reproduce the changes in blood concentrations of midazolam after intravenous and oral administration with co-administration of simeprevir at the dose of 150 mg. The reported nominal half-maximal inhibitory concentration ($IC_{50}$) of simeprevir against CYP3A4 determined by in vitro experiments using human liver microsomes was used as an initial value.[21]

## DDI analysis of simeprevir and atorvastatin

The changes in blood concentration-time profiles of atorvastatin, a dual substrate of CYP3A4 and OATP1B, after co-administration of simeprevir at the dose of 150 mg q.d. were also evaluated in healthy subjects.[5] The PBPK model structure and parameters of atorvastatin are shown in Figure 1c and Table S2. The model structure of the intestinal tract was changed from the first-order absorption model used in the previous study to the $Q_{gut}$ model to consider the inhibitory effect of simeprevir on intestinal CYP3A4.[22] Each liver compartment was divided into extrahepatic and hepatocellular compartments to incorporate the hepatic uptake process mediated by OATP1B. The model also accounted for enterohepatic recirculation because atorvastatin was excreted into bile as the unchanged drug.[23] The $k_a$, $CL_{int,all}$, and $Y_{Kp}$ were optimized simultaneously to reproduce the time course of atorvastatin blood concentration in the absence of simeprevir. Then, $K_{i,CYP3A4}$ was set at the value estimated in the analysis of DDI with midazolam, and the $K_{i,OATP1B}$ was estimated to reproduce the increase of atorvastatin blood concentration with co-administration of simeprevir at the dose of 150 mg. The experimentally determined $IC_{50}$ value of simeprevir against OATP1B using expression cell system was used as an initial value.[7]

## Analysis of interactions between simeprevir and CP-I

The effect of simeprevir multiple dose (150 mg q.d.) on CP-I plasma levels was assessed in a phase III clinical trial for the evaluation of long-term efficacy and safety in subjects with HCV.[6,7] The PBPK model structure and parameters of CP-I are shown in Figure 1d and Table S2. The membrane limited hepatic uptake by OATP1B and enterohepatic circulation were considered as well as simeprevir and atorvastatin.[22,24] The study outline of an actual clinical trial and virtual clinical trials evaluating the increase in plasma CP-I concentration by simeprevir are summarized in Table S3. The dosing amount of simeprevir, dosing duration, the total number of subjects, and the proportion of subjects with each METAVIR fibrosis score among all subjects were set at the same condition in actual and virtual clinical trials. Approximately one-third of subjects had METAVIR fibrosis score of F1 (mild fibrosis). Another one-third had fibrosis score of F2 (significant fibrosis), and the rest had fibrosis score of F3 (severe fibrosis) or F4 (cirrhosis).[6] It has been reported that the progression of liver fibrosis resulted in altering the expression levels of CYP3A4 and OATP1B,[8] which may affect the exposures of simeprevir and CP-I. Therefore, the decrease in the expression level of CYP3A4 and OATP1B in subjects with HCV with each METAVIR fibrosis score and its interindividual variations were incorporated to conduct the Monte Carlo simulation. $V_{max,CYP3A4}$ and $V_{max,OATP1B}$ for simeprevir in subjects with HCV were calculated by multiplying those in HVs and ratio of expression level in subjects with HCV to HVs. Similar to that, an active uptake intrinsic clearance on sinusoidal membrane mediated by OATP1B for CP-I in subjects with HCV was obtained by multiplying that in HVs and ratio of expression level in subjects with HCV to HVs. The interindividual variability in the renal clearance of CP-I was also considered and assumed to be comparable between healthy and HCV subjects (Table S4).[25] The interindividual variabilities of other parameters were not considered in the present study. The synthesis of CP-I was assumed to be constant between HVs and subjects with HCV. Because both simeprevir and CP-I were low systemic clearance substances,[1,22] the change in hepatic blood flow and its variability might have limited impact on study outcomes. Plasma samples were collected immediately before ($C_{\mathrm{trough}}$) and 1–7 hours after dose at 2, 4, 8, and 12 weeks after the initial dose in the actual clinical study, whereas plasma samples were collected immediately before and 2 hours after dose at 2 and 12 weeks after the initial dose in the virtual clinical study (Table S3). The reasons for adopting the simplified blood sampling in virtual clinical trials are described in the Results section. Six virtual clinical trials were performed with the fixed $K_{\mathrm{i,OATP1B}}$ that was estimated from drug interaction with atorvastatin, and compared to an actual clinical trial.

## Software

The parameter estimation and simulation were conducted by Phoenix WinNonLin version 8.1 (Certara USA). The weight for the nonlinear least-squares calculation was set as the square root of the observed value. The $P_{\mathrm{eff}}$ was predicted by ADMET predictor version 9.5 (Simulation Plus) for simeprevir and atorvastatin. The generation of virtual patient populations was performed with R version 4.2.0, as described previously.[26]

# RESULTS

## PBPK model development to describe nonlinear pharmacokinetics of simeprevir

The observed blood concentration-time profiles between 50 mg and 600 mg simeprevir doses in healthy subjects was captured well by optimizing $P_{\mathrm{eff}}$ and AR (Figure 2). These parameters were converged with small coefficient of variation (CV) values of 7.04 and 2.79%, respectively. The fixed and optimized PBPK model parameters of simeprevir are shown in Table 1 and the physiological parameters in Table S1. The observed and optimized blood AUC and maximum plasma concentration ($C_{\mathrm{max}}$) of simeprevir were summarized in Figure S1.

## Increase in midazolam exposure via CYP3A4 inhibition by simeprevir in healthy subjects

Midazolam blood concentrations after intravenous and oral administration alone can be reproduced by optimizing $k_a$, $\mathrm{CL}_{\mathrm{int,all}}$, and $Y_{\mathrm{Kp}}$ (Figure 3). The fixed and optimized PBPK model parameters for midazolam are shown in Table S2. The $K_{\mathrm{i,CYP3A4}}$ of simeprevir was estimated to be 2.89 μM (CV, 23.9%) to recover the increase

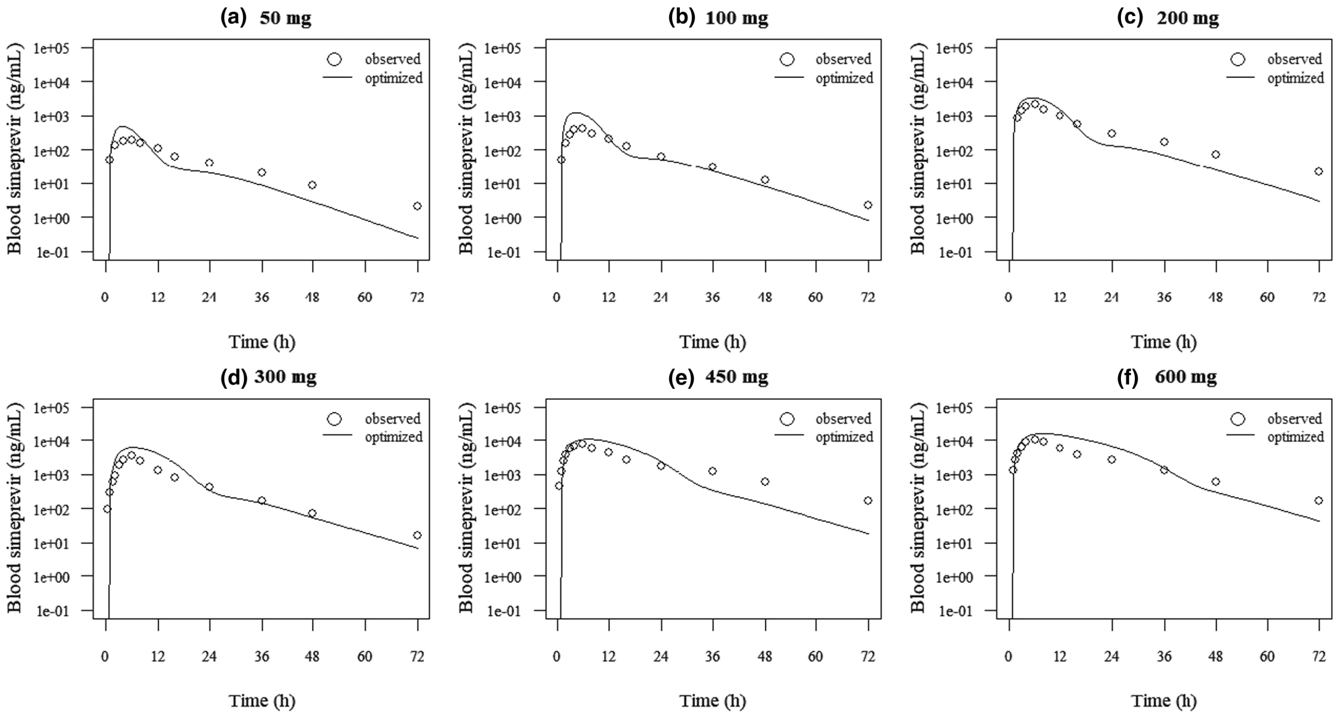

**FIGURE 2** Optimized and observed simeprevir blood concentration-time profiles after single oral administration at the doses of 50 mg (a), 100 mg (b), 200 mg (c), 300 mg (d), 450 mg (e), and 600 mg (f) in healthy volunteers. The open circles represent observed concentration-time profiles.[1] Each solid line represents an optimized concentration-time profile using PBPK model and parameters shown in Figure 1a and Table 1. PBPK, physiologically-based pharmacokinetic.

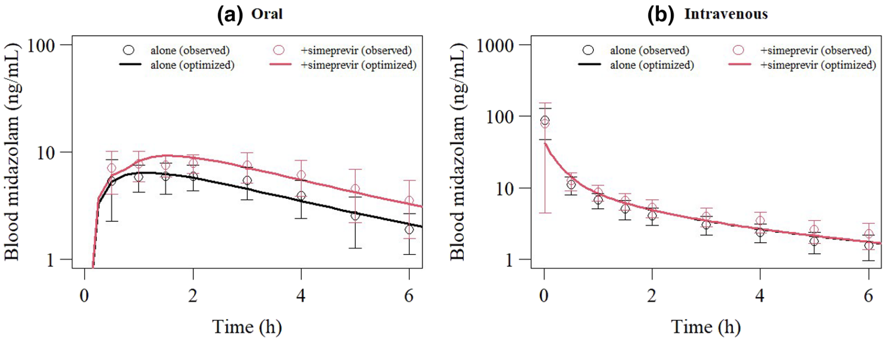

**FIGURE 3** Optimized and observed blood concentration-time profiles of oral (a) and intravenous (b) midazolam before and after simeprevir once daily oral administrations at the dose of 150 mg for 10 days (oral midazolam) and 11 days (intravenous midazolam) in healthy volunteers. Oral and intravenous midazolam were administered at the doses of 0.075 mg/kg and 0.025 mg/kg, respectively.[5] The black and red circles represent observed blood midazolam concentrations in the absence and presence of simeprevir, respectively. The circles and bars represent measured concentrations and their SD values, respectively. The black and red lines represent optimized blood midazolam concentration-time profiles in the absence and presence of simeprevir, respectively.

**TABLE 2** Observed and optimized fold increase in AUC and $C_{max}$ of midazolam and atorvastatin following once daily multiple oral simeprevir dosing in healthy volunteers.

| | Mean ratio (90% CI) with/without simeprevir | | | |
|---|---|---|---|---|
| | $C_{max}$ | | AUC | |
| Victim drug | Observed | Simulated | Observed | Simulated |
| Midazolam (i.v.) | 0.78 (0.52–1.17) | 1.00 | 1.10 (0.95–1.26) | 1.00 |
| Midazolam (p.o.) | 1.31 (1.19–1.45) | 1.46 | 1.45 (1.35–1.57) | 1.49 |
| Atorvastatin (p.o.) | 1.70 (1.42–2.04) | 2.69 | 2.12 (1.72–2.62) | 2.38 |

*Note*: Midazolam was administered at the doses of 0.075 mg/kg orally and 0.025 mg/kg intravenously. Atorvastatin was administered orally at the dose of 40 mg. Simeprevir was administered at the dose of 150 mg for 11 days for intravenous midazolam and 10 days for oral midazolam and atorvastatin.[5]

Abbreviations: AUC, area under the concentration-time curve; CI, confidence interval; $C_{max}$, maximum plasma concentration.

in oral midazolam exposure in the presence of simeprevir (Table 1). Simulated $C_{max}$ and AUC fold-increase in oral midazolam exposure by simeprevir dosing were 1.46 and 1.49-fold, whereas those observed in the clinical study were 1.31 and 1.45-fold, respectively.[5] On the other hand, co-administration of simeprevir showed no apparent change in intravenous midazolam exposure. These results were in line with observed data (Table 2 and Figure 3).

## Increase in atorvastatin exposure via CYP3A4 and OATP1B inhibition of simeprevir in healthy subjects

A blood concentration–time profile of atorvastatin in the absence of concomitant drugs was reproduced by optimizing $k_a$, $CL_{int,all}$, and $Y_{Kp}$ (Figure 4). The fixed and optimized PBPK model parameters of atorvastatin are shown in Table S2. When $K_{i,CYP3A4}$ was set at the value obtained by the analysis of DDI with midazolam (2.89 μM), $K_{i,OATP1B}$ was estimated to be 0.00347 μM (CV, 6.73%) to recover the increase in atorvastatin exposure by coadministration of

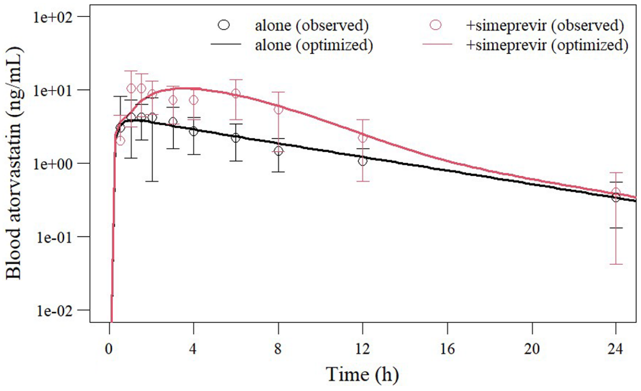

**FIGURE 4** Optimized and observed blood concentration-time profiles of atorvastatin before and after simeprevir once daily oral administrations at the dose of 150 mg for 10 days in healthy volunteers. Atorvastatin was administered orally at the dose of 40 mg.[5] The black and red circles represent observed blood atorvastatin concentration in the absence and presence of simeprevir, respectively. The circles and bars represent measured concentrations and their SD values, respectively. The black and red lines represent optimized blood atorvastatin concentration-time profiles in the absence and presence of simeprevir, respectively.

simeprevir (Table 1). The simulated increase in atorvastatin $C_{max}$ and AUC were 2.69 and 2.38-fold, whereas those observed in the clinical study were 1.70 and 2.12-fold, respectively (Table 2 and Figure 4).[5]

## Relationship between simeprevir and CP-I blood concentrations in subjects with HCV

When $K_{i,OATP1B}$ was set at the value estimated by the analysis of DDIs with atorvastatin (0.00347 μM), a total of six virtual clinical trials of the same size as the clinical trial were conducted, and the results are shown in Figure 5. When conducting virtual clinical studies, decreases in expression levels of hepatic CYP3A4 and OATP1B in subjects with HCV with each METAVIR fibrosis score compared to healthy subjects were considered. In addition, interindividual variabilities for hepatic CYP3A4 expression level, OATP1B expression level,[8,27] and CP-I renal clearance were also incorporated (Table S4).[24] The CP-I blood concentrations were in a similar range around 0.6 nM when the simeprevir blood concentration were below ~2000 ng/mL, and then increased up to 6 nM at the simeprevir blood concentration range from 2000 to 30,000 ng/mL in the actual clinical trial (Figure 5a).[7] All virtual clinical trials adequately predicted this trend (Figure 5b–h). Simulation results indicated that some subjects with METAVIR fibrosis scores of F1 and F2 showed CP-I concentrations around the baseline, whereas many of F3 and F4 subjects showed high blood concentrations of both simeprevir and CP-I.

Besides the phase III clinical trial investigating the relationship between CP-I and simeprevir, the plasma concentration-time profile of simeprevir in representative subjects with HCV (METAVIR fibrosis score not assigned) was also reported.[21] The observed and simulated blood concentration-time profiles after single oral administration of simeprevir at the doses of 75 mg, 150 mg, and 200 mg in representative patients with HCV are shown in Figure S2. The simulated blood concentration-time profiles in subjects with HCV with METAVIR fibrosis scores of F1 and F2, who accounted for 67% among all participants in the phase III clinical trial, seemed to capture the observed data in representative subjects with HCV. The simulated concentrations of unbound simeprevir in liver sinusoids, hepatocytes, and enterocytes at steady-state after once-daily oral administration of simeprevir at the dose of 150 mg for 12 weeks are shown in Figure S3. The optimized $K_{i,CYP3A4}$ and $K_{i,OATP1B}$ are overlaid.

## DISCUSSION

In this study, a series of DDIs of simeprevir as a perpetrator were analyzed by PBPK modeling coupled with Monte

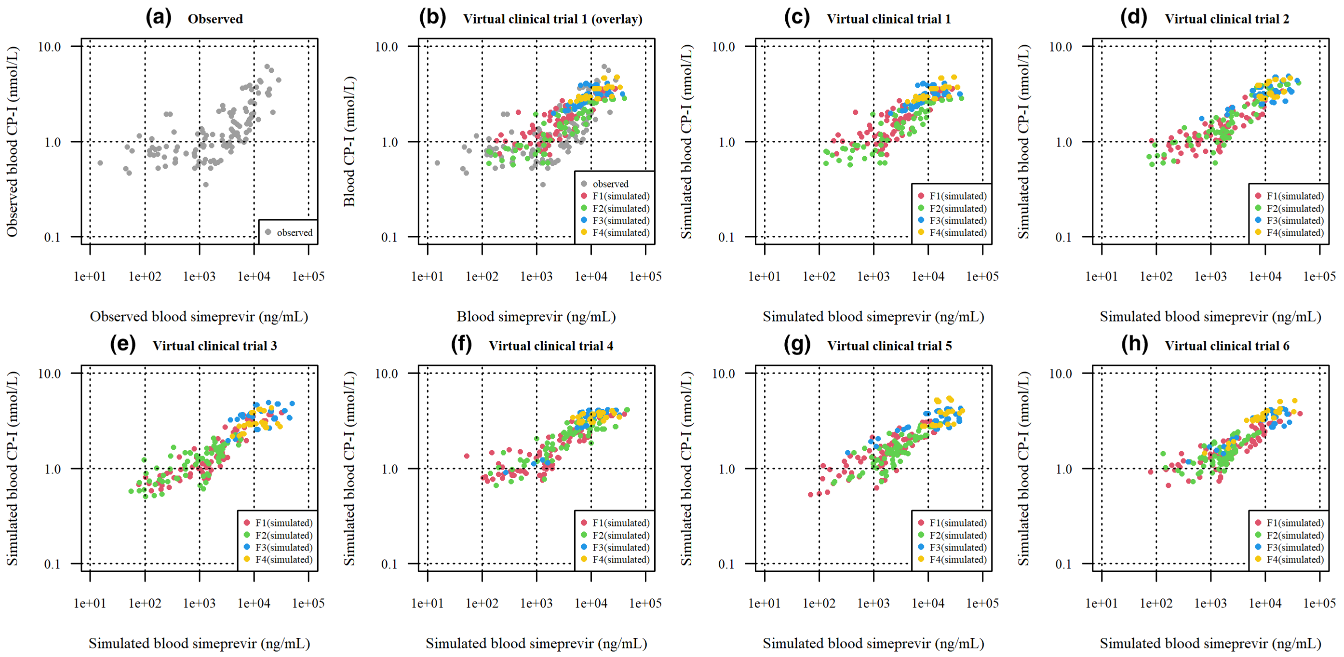

**FIGURE 5** Observed (a) and simulated (b–h) relationship between blood concentrations of CP-I and simeprevir in subjects with HCV. Gray circles represent observed data. Red, green, blue, and yellow circles represent and simulated data in subjects with HCV with METAVIR fibrosis score F1, F2, F3, and F4, respectively. Simeprevir was orally administered once daily at the dose of 150 mg.[7] Plasma samples were prepared from 2 to 12 weeks after first dose. Detailed study conditions were shown in Table S3. CP-I, coproporphyrin-I; HCV, hepatitis C virus.

Carlo simulation to estimate and verify the in vivo $K_i$ of simeprevir against CYP3A4 and OATP1B.

Because it has been reported that the saturation of CYP3A4 metabolism and hepatic uptake mediated by OATP1B contributed the nonlinear pharmacokinetics of simeprevir, a PBPK model structure, including CYP3A4 metabolism in the small intestine and liver, hepatic uptake by OATP1B was adopted.[1,4,28] The model also accounted for enterohepatic recirculation because simeprevir was excreted into bile as the unchanged drug (Figure 1a).[21] The values of parameters related to drug systemic clearance, such as $CL_{int,all}$, $V_{max}$, and $K_m$ were obtained from the previous reports.[1,4] The concentration-time profiles of simeprevir at the doses from 50 to 600 mg in healthy subjects were reproduced by optimizing two parameters related to intestinal absorption, $P_{eff}$ and AR (Figure 2 and Table 1). If AR was fixed to be unity and only $P_{eff}$ was optimized, nonlinear pharmacokinetics of simeprevir was also adequately captured (data not shown). These results indicated that AR had limited impact on nonlinearity in this case, but $K_m$ for OATP1B and CYP3A4 were key parameters to capture the nonlinearity.

The reported PBPK model structure of midazolam was used in this study.[9] By optimizing $k_a$, $CL_{int,all}$, and $Y_{Kp}$ of midazolam, the time course of blood midazolam concentration without concomitant use of simeprevir was reproduced. It has been reported that simeprevir shows the competitive inhibition against CYP3A4, but not time-dependent inhibition.[21] The unbound $K_{i,CYP3A4}$ was estimated to be 2.89 μM with the reasonable CV value of 23.9% using PBPK model analysis (Table 1 and Figure 3). Simulated unbound simeprevir concentrations in enterocyte compartment exceeded the optimized unbound $K_{i,CYP3A4}$ up to 6–8 h postdose, indicating the inhibition of intestinal CYP3A4 activity by simeprevir. On the other hand, simeprevir was unlikely inhibit the hepatic CYP3A4 in hepatocytes because the simulated unbound simeprevir concentrations in hepatocytes were 100-fold lower than $K_{i,CYP3A4}$ over the entire dosing interval (Figure S3b,c). These were consistent with the observation that coadministration of simeprevir increased the exposure of orally administered midazolam but had little effect on the exposure of intravenously administered midazolam.[5] As a result of in vitro study using human liver microsomes, the nominal $IC_{50}$ values of simeprevir were determined to be 84.5 and 153 μM for 4- and 1′-midazolam hydroxylase activities, respectively.[21] By considering the unbound fraction in incubation determined by in vitro binding experiments, unbound $IC_{50}$ was estimated to be 0.455–0.823 μM. $K_{i,CYP3A4}$ obtained by the PBPK model analysis (2.89 μM) was not significantly different from the range of inhibitory concentration determined in the in vitro studies.

The model structure of the intestinal absorption of atorvastatin was modified from the previously reported first-order absorption to the $Q_{gut}$ model to incorporate CYP3A4 metabolism in the enterocytes, enabled us to consider the inhibition of intestinal CYP3A4 activity by simeprevir. The PBPK model structure and values of parameters related distribution, metabolism, and excretion of atorvastatin were obtained from the previous reports (Figure 1c and Table S2).[22] When unbound $K_{i,CYP3A4}$ was set at the value obtained by the PBPK analysis with midazolam (2.89 μM), unbound $K_{i,OATP1B}$ was estimated to be 0.00347 μM with the small CV value of 6.73% (Table 1 and Figure 4). The simulated unbound $C_{max}$ of simeprevir in the liver sinusoid compartment exceeded $K_{i,OATP1B}$ in healthy subjects (Figure S3a). The nominal $IC_{50}$ values of simeprevir against OATP1B1 and 1B3 determined by the expression cell system were reported to be 0.7 and 0.6 μM, respectively.[7] These values were ~200-fold higher than unbound $K_{i,OATP1B}$ estimated by the PBPK model analysis (0.00347 μM), possibly due to high nonspecific binding to cellular components and experimental materials. On the other hand, the $K_{m,OATP1B}$ of simeprevir estimated by PBPK model analysis was reported to be 0.003 μM,[1] which was close to $K_{i,OATP1B}$ obtained in this study.

The reported PBPK model structure and parameters of CP-I constructed by authors (Sugiyama and his co-workers) were used in this study (Figure 1d and Table S2).[22,24] Blood samples were collected at multiple timepoints up to 7 h after dose at 2, 4, 8, and 12 weeks in the actual clinical trial. However, sampling points were set at 0 and 2 h after the dose, corresponding to trough and peak concentrations, at 2 and 12 weeks in the virtual clinical trials. The reasons for these differences are (1) blood sampling timepoints at 0 and 2 h postdose accounted for 70% of total samples, (2) ~40% of samples were collected at week 2, followed by 12 weeks (Table S5), (3) the blood concentrations of simeprevir and CP-I seemed to be a similar range across entire weeks, indicating that those of both substances reached steady-state at week 2 in the actual clinical study (Figure S4). The highest blood simeprevir concentration was 28,400 ng/mL among all samples collected from the actual clinical trial in subjects with HCV, whereas average $C_{max}$ at steady-state in healthy volunteers was only 2350 ng/mL,[1] despite of the same dose amount of 150 mg. This was likely due to decrease in drug clearance in subjects with HCV compared to healthy subjects. Therefore, in the virtual clinical trials, the extent of decrease in hepatic CYP3A4 and OATP1B expression levels in response to each METAVIR fibrosis score were incorporated (Table S4). The mRNA levels of CYP3A4 and OATP1B in liver biopsy samples collected from subjects with HCV with METAVIR fibrosis scores of F1, F2, and F3 were measured and found that both mRNA levels were decreasing with progressing the fibrosis state.[8] For F4 subjects (liver cirrhosis), the reported CYP3A4 and OATP1B protein abundances in liver biopsy samples collected from subjects with cirrhotic liver were incorporated.[27] In this proteomics study, protein abundances of CYP3A4 and OATP1B were evaluated in patients with Child-Pugh classes A, B, and C. Because the efficacy and safety study of simeprevir has not been conducted in HCV-infected patients with Child-Pugh class B and C,[29] the reported values from subjects with Child-Pugh class A were used. Because variabilities in CYP3A4 and OATP1B were not statistically significant among all METAVIR fibrosis scores from F1 to F4, the observed average CV% was used in simulations. In addition, interindividual variability of the CP-I renal clearance was also considered and assumed that the variability in subjects with HCV was comparable to that in healthy subjects.[25] The results of a total of six virtual clinical trials when the $K_{\mathrm{i,OATP1B}}$ was set at the value estimated by the DDI analysis with atorvastatin (0.00347 μM) are shown in Figure 5. In the actual clinical trial, blood CP-I concentration increased when blood simeprevir concentrations exceed 2000 ng/mL (2.67 μM), and maximum CP-I concentration reached around 6 nM. Comparable relationships between simeprevir and CP-I blood levels were successfully predicted in all virtual clinical trials relative to the actual clinical trial, despite that no parameter optimization to match observed data was conducted. Our simulations showed that blood concentrations of both substances tended to be higher in subjects with severe hepatic impairment (F3 and F4), due to low drug clearances and potent OATP1B inhibition by simeprevir. These simulations clearly demonstrated that PBPK model analysis coupled with Monte Carlo simulation to consider the interindividual variability in drug metabolizing enzymes and transporters was a useful approach to describing and understanding complex DDI cases.

Simeprevir showed the inhibitory potency against multidrug resistance-associated protein 2 (MRP2) with the $\mathrm{IC}_{50}$ of 6.4 μM (4800 ng/mL) in vitro.[30] CP-I was a substrate of MRP2 as well as OATP1B.[7] Therefore, MRP2 inhibition by simeprevir might be involved in the increase in CP-I blood levels. However, simulated unbound simeprevir $C_{\max}$ in hepatocytes (~30 ng/mL) was much lower than the nominal $\mathrm{IC}_{50}$, suggesting that the MRP2 inhibition by simeprevir may not contribute to the interaction between simeprevir and CP-I. In fact, if the $K_{\mathrm{i,MRP2}}$ value were set at 1000-fold lower than the nominal $\mathrm{IC}_{50}$, the minimal impact on blood CP-I concentration was simulated using constructed PBPK models (data not shown).

In conclusion, in vivo $K_{\mathrm{i,CYP3A4}}$ and $K_{\mathrm{i,OATP1B}}$ were estimated sequentially by the PBPK modeling approach using DDI cases with midazolam and atorvastatin in healthy subjects. Then, optimized $K_{\mathrm{i,OATP1B}}$ was verified in the interaction with CP-I by PBPK model analysis coupled with Monte Carlo simulation to incorporate the interindividual variability in hepatic CYP3A4 and OATP1B expression levels in subjects with HCV in this study. This study has demonstrated that PBPK model analysis can reasonably describe the drug–drug and -endogenous biomarker interactions even when the drug-disease interactions are also involved in the study outcomes.

## AUTHOR CONTRIBUTIONS

S.N., K.T., S.Y., J.S., and Y.S. wrote the manuscript. S.N., K.T., and Y.S. designed the research. S.N., K.T., and Y.S. performed the research. S.N., and Y.S. analyzed the data.

## ACKNOWLEDGMENTS

The authors thank Takashi Yoshikado (Yokohama University of Pharmacy) and Ryuta Asaumi (Astellas Pharma Inc.) for providing model code.

## FUNDING INFORMATION

No funding was received for this work.

## CONFLICT OF INTEREST STATEMENT

The authors declared no competing interests for this work.

## ORCID

*Shinji Yamazaki* https://orcid.org/0000-0001-7112-2812

## REFERENCES

1. Snoeys J, Beumont M, Monshouwer M, Ouwerkerk-Mahadevan S. Mechanistic understanding of the nonlinear pharmacokinetics and intersubject variability of simeprevir: a PBPK-guided drug development approach. *Clin Pharmacol Ther.* 2016;99(2):224-234.
2. Snoeys J, Beumont M, Monshouwer M, Ouwerkerk-Mahadevan S. Elucidating the plasma and liver pharmacokinetics of simeprevir in special populations using physiologically based pharmacokinetic modelling. *Clin Pharmacokinet.* 2017;56(7):781-792.
3. Ouwerkerk-Mahadevan S, Snoeys J, Simion A, Scheers E, Beumont M. A novel microdose approach to assess bioavailability, intestinal absorption, gut metabolism, and hepatic clearance of simeprevir in healthy volunteers. *Presented at the 15th International Workshop on Clinical Pharmacology of HIV and Hepatitis Therapy*. 2014.
4. Yoshikado T, Maeda K, Kusuhara H, Furihata K, Sugiyama Y. Quantitative analyses of the influence of parameters governing rate-determining process of hepatic elimination of drugs on the magnitudes of drug–drug interactions via hepatic OATPs and CYP3A using physiologically based pharmacokinetic models. *J Pharm Sci.* 2017;106(9):2739-2750.

5. Ouwerkerk-Mahadevan S, Snoeys J, Peeters M, Beumont-Mauviel M, Simion A. Drug–drug interactions with the NS3/4A protease inhibitor Simeprevir. *Clin Pharmacokinet.* 2016;55(2):197-208.
6. Forns X, Lawitz E, Zeuzem S, et al. Simeprevir with peginterferon and ribavirin leads to high rates of SVR in patients with HCV genotype 1 who relapsed after previous therapy: a phase 3 trial. *Gastroenterology.* 2014;146(7):1669-1679.
7. Kunze A, Ediage EN, Dillen L, Monshouwer M, Snoeys J. Clinical investigation of coproporphyrins as sensitive biomarkers to predict mild to strong OATP1B-mediated drug–drug interactions. *Clin Pharmacokinet.* 2018;57(12):1559-1570.
8. Nakai K, Tanaka H, Hanada K, et al. Decreased expression of cytochromes P450 1A2, 2E1, and 3A4 and drug transporters Na+−taurocholate-cotransporting polypeptide, organic cation transporter 1, and organic anion-transporting peptide-C correlates with the progression of liver fibrosis in chronic hepatitis C patients. *Drug Metab Dispos.* 2008;36(9):1786-1793.
9. Asaumi R, Toshimoto K, Tobe Y, et al. Comprehensive PBPK model of rifampicin for quantitative prediction of complex drug–drug interactions: CYP3A/2C9 induction and OATP inhibition effects. *CPT Pharmacometrics Syst Pharmacol.* 2018;7(3):186-196.
10. Asaumi R, Menzel K, Lee W, et al. Expanded physiologically-based pharmacokinetic model of rifampicin for predicting interactions with drugs and an endogenous biomarker via complex mechanisms including organic anion transporting polypeptide 1B induction. *CPT Pharmacometrics Syst Pharmacol.* 2019;8(11):845-857.
11. Asaumi R, Nunoya KI, Yamaura Y, Taskar KS, Sugiyama Y. Robust physiologically based pharmacokinetic model of rifampicin for predicting drug–drug interactions via P-glycoprotein induction and inhibition in the intestine, liver, and kidney. *CPT Pharmacometrics Syst Pharmacol.* 2022;11(7):919-933.
12. Yao Y, Toshimoto K, Kim SJ, Yoshikado T, Sugiyama Y. Quantitative analysis of complex drug–drug interactions between cerivastatin and metabolism/transport inhibitors using physiologically based pharmacokinetic modeling. *Drug Metab Dispos.* 2018;46(7):924-933.
13. Kim SJ, Toshimoto K, Yao Y, Yoshikado T, Sugiyama Y. Quantitative analysis of complex drug–drug interactions between repaglinide and cyclosporin a/gemfibrozil using physiologically based pharmacokinetic models with In vitro transporter/enzyme inhibition data. *J Pharm Sci.* 2017;106(9):2715-2726.
14. Nishiyama K, Toshimoto K, Lee W, Ishiguro N, Bister B, Sugiyama Y. Physiologically-based pharmacokinetic Modeling analysis for quantitative prediction of renal transporter-mediated interactions between metformin and cimetidine. *CPT Pharmacometrics Syst Pharmacol.* 2019;8(6):396-406.
15. Hisaka A, Ohno Y, Yamamoto T, Suzuki H. Prediction of pharmacokinetic drug–drug interaction caused by changes in cytochrome P450 activity using in vivo information. *Pharmacol Ther.* 2010;125(2):230-248.
16. Toshimoto K, Tomaru A, Hosokawa M, Sugiyama Y. Virtual clinical studies to examine the probability distribution of the AUC at target tissues using physiologically-based pharmacokinetic modeling: application to analyses of the effect of genetic polymorphism of enzymes and transporters on irinotecan induced side effects. *Pharm Res.* 2017;34(8):1584-1600.
17. Watanabe T, Kusuhara H, Maeda K, Shitara Y, Sugiyama Y. Physiologically based pharmacokinetic modeling to predict transporter-mediated clearance and distribution of pravastatin in humans. *J Pharmacol Exp Ther.* 2009;328(2):652-662.
18. Cong D, Doherty M, Pang KS. A new physiologically based, segregated-flow model to explain route-dependent intestinal metabolism. *Drug Metab Dispos.* 2000;28(2):224-235.
19. Rodgers T, Leahy D, Rowland M. Physiologically based pharmacokinetic modeling 1: predicting the tissue distribution of moderate-to-strong bases. *J Pharm Sci.* 2005;94(6):1259-1276.
20. Rodgers T, Rowland M. Physiologically based pharmacokinetic modelling 2: predicting the tissue distribution of acids, very weak bases, neutrals and zwitterions. *J Pharm Sci.* 2006;95(6):1238-1257.
21. Center for Drug Evaluation and Research, FDA. Pharmacology Review(s). https://www.accessdata.fda.gov/drugsatfda_docs/nda/2013/205123Orig1s000PharmR.pdf
22. Yoshikado T, Toshimoto K, Maeda K, et al. PBPK modeling of coproporphyrin I as an endogenous biomarker for drug interactions involving inhibition of hepatic OATP1B1 and OATP1B3. *CPT Pharmacometrics Syst Pharmacol.* 2018;7(11):739-747.
23. Lennernäs H. Clinical pharmacokinetics of atorvastatin. *Clin Pharmacokinet.* 2003;42(13):1141-1160.
24. Yoshikado T, Aoki Y, Mochizuki T, et al. Cluster Gauss-Newton method analyses of PBPK model parameter combinations of coproporphyrin-I based on OATP1B-mediated rifampicin interaction studies. *CPT Pharmacometrics Syst Pharmacol.* 2022;11(10):1341-1357.
25. Feng S, Bo Q, Coleman HA, et al. Evaluation of coproporphyrins as clinical endogenous markers for OATP1B. *J Clin Pharmacol.* 2021;61(8):1027-1034.
26. Nakamura T, Toshimoto K, Lee W, Imamura CK, Tanigawara Y, Sugiyama Y. Application of PBPK modeling and virtual clinical study approaches to predict the outcomes of CYP2D6 genotype-guided dosing of tamoxifen. *CPT Pharmacometrics Syst Pharmacol.* 2018;7(7):474-482.
27. El-Khateeb E, Achour B, Al-Majdoub ZM, Barber J, Rostami-Hodjegan A. Non-uniformity of changes in drug-metabolizing enzymes and transporters in liver cirrhosis: implications for drug dosage adjustment. *Mol Pharm.* 2021;18(9):3563-3577.
28. Toshimoto K, Fukuchi Y, Aoki Y, Sugiyama Y. Middle-out approach for PBPK modeling using cluster Gauss-Newton method: application to the nonlinear pharmacokinetics analysis of simeprevir. *Presented at the 36th Annual Meeting of the Japanese Society for the Study of Xenobiotics (JSSX).* 2021.
29. Center for Drug Evaluation and Research, FDA. Prescribing Information. https://www.accessdata.fda.gov/drugsatfda_docs/label/2013/205123s001lbl.pdf
30. Huisman MT, Snoeys J, Monbaliu J, Martens M, Sekar V, Raoof A. In vitro studies investigating the mechanism of interaction between TMC435 and hepatic transporters. *Presented at the 61st Annual Meeting of the American Association for the Study of Liver Disease (AASLD).* 2010.
31. Ring BJ, Chien JY, Adkison KK, et al. PhRMA CPCDC initiative on predictive models of human pharmacokinetics, part 3: comparative assessment of prediction methods of human clearance. *J Pharm Sci.* 2011;100(10):4090-4110.

32. Center for Drug Evaluation and Research, FDA. In vitro drug interaction studies – cytochrome P450 enzyme- and transporter-mediated drug interactions guidance for industry. 2020.

## SUPPORTING INFORMATION

Additional supporting information can be found online in the Supporting Information section at the end of this article.

**How to cite this article:** Nakayama S, Toshimoto K, Yamazaki S, Snoeys J, Sugiyama Y. Physiologically-based pharmacokinetic modeling for investigating the effect of simeprevir on concomitant drugs and an endogenous biomarker of OATP1B. *CPT Pharmacometrics Syst Pharmacol*. 2023;12:1461-1472. doi:10.1002/psp4.13023